



Synthesis and characterization of in situ cross-linked hydrogel based on self-assembly of thiol-modified chitosan with PEG diacrylate using Michael type addition

Da-yong Teng^{a,1}, Zhong-ming Wu^{b,1}, Xin-ge Zhang^{a,*}, Yan-xia Wang^a, Chao Zheng^a, Zhen Wang^a, Chao-xing Li^{a,*}

^aThe Key Laboratory of Functional Polymer Materials of Ministry Education, Institute of Polymer Chemistry, Nankai University, Tianjin 300071, China

^bMetabolic Diseases Hospital, Tianjin Medical University, Tianjin 300070, China

ARTICLE INFO

Article history:

Received 24 February 2009

Received in revised form

16 November 2009

Accepted 7 December 2009

Available online 4 January 2010

Keywords:

Chitosan

In situ hydrogel

Michael type addition

ABSTRACT

A novel injectable in situ cross-linked hydrogel has been designed via Michael type addition between thiol-modified chitosan (CS–NAC) and PEG diacrylate (PEGDA). Hydrogel was rapidly formed in situ under physiological conditions. The gelation time depended on the content of free thiols in CS–NAC, temperature, and concentration of CS–NAC and PEGDA. Thermogravimetric analysis showed the thermal stabilities of hydrogels. SEM observation results confirmed a porous 3D structure. Rheological studies showed that the cross-linking density and elasticity of hydrogel had a correlation to the content of CS–NAC and PEGDA. Swelling studies revealed that these hydrogels had a high initial swelling and were degradable under physiological conditions. And swelling was highly temperature-dependent and was directly related to the amount of cross-linking. Biological activities of the hydrogels were evaluated by *in vitro* cell compatibility on HDFs and A549 cells and the results indicated that the hydrogel was biocompatible.

© 2009 Elsevier Ltd. All rights reserved.

1. Introduction

Hydrogels are three-dimensional cross-linked polymer networks, which may absorb from 10% to 20% up to thousands of times their dry weight in water, giving them physical characteristics similar to soft tissues. Due to their excellent biocompatibility, causing minimal inflammatory responses, thrombosis and tissue damage, many hydrogels have been studied extensively for biomedical applications [1,2], such as drug delivery [3] and tissue engineering [4,5]. Hydrogels that are injectable and can be formed in situ under physiological conditions have received much attention recently because of their many favorable characteristics. For instance, injectable materials can conform to complex shapes at the site of injury, and can strongly adhere to the tissue during gelation. Furthermore, in situ gelation allows minimize the invasiveness of the surgical technique by permitting the use of injection or laparoscopic methods. During the last decade, many

potential applications have been explored for ideal injectable in situ crosslinkable hydrogels [6–10].

In situ gelation can be obtained after UV-polymerization [11], introducing non-reversible covalent bonds, or via self-assembly by either reversible interactions or non-reversible chemical reactions [12–19]. Among these in situ gelling systems, self-assembling hydrogels which can be formed in time or in response to a certain stimulus are of great interest. Both physical interactions, such as electrostatic [12–14] or hydrophobic interactions [15–17], as well as end-group-specific chemical reactions, such as Michael addition [18,19], can be exploited for the design of self-assembly polymeric networks. However, physically cross-linked hydrogels are generally mechanically weaker than chemically cross-linked hydrogels. Therefore, in situ gelation hydrogels prepared via Michael addition between thiols and acrylates have received much attention recently. The reaction can be carried out under physiological conditions and biomimetic scaffolds can be easily obtained by incorporation of thiol-bearing molecules. Hubbell et al. reported the hydrogels by Michael type addition between small molecules bearing several thiol groups and multi-arm star PEG acrylates or vinyl sulfones [20–22]. The experiments suggest that the cells can secrete extracellular matrix that can adhere to the hydrogels, although the PEG materials resist protein adsorption. Prestwich et al. synthesized hydrogels by Michael type addition between

* Corresponding authors. Tel.: +86 22 2350 1645; fax: +86 22 2350 5598.

E-mail addresses: zhangxing@nankai.edu.cn (X.-g. Zhang), lcx@nankai.edu.cn (C.-x. Li).

¹ Da-yong Teng contributed equally with Zhong-ming Wu, and they are the co-first authors for this paper.

thiol-modified hyaluronic acid (HA), a major nonsulfated glucosaminoglycan constituent of extracellular matrix (ECM), and PEG diacrylate [23–25]. These injectable synthetic ECM (sECM) hydrogels had very high water content (>96%), biodegradability, mechanical properties, and gelation times (~2–6 min) suitable for potential clinical applications. In addition, Hiemstra et al. prepared hydrogels via Michael type addition between thiol-modified dextran and PEG tetra-acrylate or dextran vinyl sulfone conjugate [26–28]. The results indicate that these hydrogels are very promising for use in biomedical applications, since they can be rapidly formed *in situ* and are biodegradable with adjustable degradation times to match a particular application.

It is well known that chitosan (CS) is a natural polysaccharide which has been widely used in pharmaceutical areas thanks to its attractive biocompatibility, biodegradability, antimicrobial activity, retention of growth factors, release of glucosamine and *N*-acetylglucosamine monomers and oligomers, and stimulation of cellular activities [29–31]. Modified CS has been administered to humans in the form of dressings for wounded soft and bone tissues [32,33], such as articular cartilage [34]. In particular, PEG-modifying CS with thermo-sensitive properties improves blood compatibility of CS, and also decreases the enzyme degradation, which is of great interest in drug delivery and tissue engineering [35–38]. Insup et al. synthesized a novel chitosan-PEO *in situ* hydrogel via grafting of 2-carboxyethyl acrylate to CS and Michael addition reaction was processed between acrylate modified CS and PEO hexa-thiols [39]. However, the thermo-sensitive properties of the hydrogel were not presented. In this paper, a novel *in situ* cross-linked hydrogel that was formed under physiological conditions by Michael type addition between thiol-modified CS and PEG diacrylate was prepared. Moreover, gelation time, mechanical properties, thermally swelling properties and *in vitro* cell compatibility of the hydrogels were characterized.

2. Experimental

2.1. Materials

Chitosan (degree of deacetylation 86%, with molecular mass of 300 kDa) was purchased from the Zhejiang Yuhuan Ocean Biochemical Co., Ltd. (Zhejiang, China) and used as received. *N*-acetyl-L-cysteine (NAC), 1-ethy-3-(3-dimethyl-aminopropyl-carbodiimide) hydrochloride (EDAC·HCl), 1-hydroxybenzotriazole (HOBt), 3-[4,5-dimethylthiazol-2-yl]-2,5-diphenyltetrazolium bromide (MTT) and Ellman's reagent were obtained from the J&K China Chemical Ltd. Poly(ethylene glycol) diacrylate (PEGDA, M_w 2 kDa, degree of substitution 87%, as determined by ^1H NMR) was synthesized by PEG diol and Acryloyl chloride according to the literature [40]. All other chemicals were of analytical grade and were used without further purification.

2.2. Synthesis of chitosan-NAC

Chitosan-NAC (CS-NAC) conjugates were prepared as described by Krauland et al. [41]. Typically, 500 mg of CS was dispersed in water (46 mL), and added HOBt (348.6 mg, 2.58 mmol) to above suspension under stirring until a clear solution obtained. Afterwards, NAC (842.0 mg, 5.16 mmol) was added to the solution followed by the addition of a solution of EDAC·HCl (1978.5 mg, 10.32 mmol, 4 mL). The pH of the reaction mixture was adjusted to 5 by the addition of 1 M HCl. The reaction mixture was incubated for 3 h at room temperature under stirring. The resultant mixture was dialyzed (M_w 10000 cut) first against 5 mM HCl containing 2 μM EDTA for 3 days at 4 °C in the dark, and then the same medium but additionally containing 1% of NaCl and finally 1 mM HCl. The dialyzed fragments

were then lyophilized and stored at 4 °C until further use. Thiol group content on thiolated chitosan was determined using the Ellman's reagent as described by Krauland et al. [41].

2.3. Gelation time and swelling tests

To determine the gelation time, solutions of CS-NAC and PEGDA (molar ratios of thiol to acrylate group were 1:1, 1:2 and 1:5) in $\text{NaH}_2\text{PO}_4/\text{Na}_2\text{HPO}_4$ buffer (PBS, pH 7.4, 0.1 M) were mixed and incubated at 37 °C by vortexing. In comparison, CS-NAC was dissolved in PBS (pH 7.4, 0.1 M) at 37 °C to induce hydrogel states. The gelation time was determined by a flow test utilizing a glass test tube inverting method reported by Jeong et al. [42]. As the solution lost fluidity in 1 min, the sample was regarded as a gel. For the swelling test, the prepared hydrogels were allowed to swell and erode at 25 or 37 °C after applying 10 mL PBS. The swollen and degraded hydrogels were weighed at various time intervals after removal of PBS. After each weighing, PBS was refreshed. The swelling ratio of the hydrogels was calculated from the initial dry hydrogel weight (W_0) and the swollen hydrogel weight after exposure to PBS (W_t): Swelling ratio (%) = W_t/W_0 .

2.4. Rheological experiments

A Stress Tech rheometer (Reologica Instruments Inc.) with standard steel parallel-plate geometry of 25 mm diameter was used for the rheological characterization of all hydrogel samples (after gelation). The test methods employed were oscillatory stress sweep and frequency sweep. The stress sweep was performed on hydrogels to determine the linear viscoelastic region (LVR) profiles of them and compare the storage modulus (G') under the same physical condition. The stress sweep was set up by holding the temperature (25 °C) and frequency (1 Hz) constant while increasing the stress level from 0.1 to 100 Pa. We also subjected the hydrogels to a frequency sweep at a fixed shear stress (10 Pa) and temperature (25 °C), the oscillatory frequency was increased from 0.01 to 20 Hz and the G' was recorded. The plots of G' versus shear stress or frequency from the two sweep tests were obtained directly from the software controlling the rheometer.

2.5. Characterization of hydrogels

X-ray diffraction patterns were obtained by using a diffractometer (XRD-6000, Shimadzu) equipped with a θ - θ goniometer. The operating conditions during the experiment were 40 kV and 50 mA with Cu $K\alpha$ radiation. The diffraction patterns were acquired over a diffraction angle of $2\theta = 10$ – 30° .

To examine thermal stability of hydrogels, the hydrogel samples were measured using thermogravimetric analysis (TGA, Mettsh). Decomposition profiles of TGA were recorded with a heating rate of 10 °C/min in nitrogen between 20 and 650 °C.

To observe the interior morphologies of hydrogels, the swollen hydrogel samples were quickly frozen in liquid nitrogen and further freeze-dried in a Freeze Drier (Christ alpha2-4 LD plus, Christ) under vacuum at -90°C for at least 2 d until all the solvent was sublimed. The freeze-dried hydrogels were then fractured carefully, and the interior morphologies of the hydrogels were visualized by using a scanning electron microscope (SEM, SS-550, Shimadzu). Before the SEM observation, the hydrogel samples were fixed on aluminum stubs and coated with gold.

2.6. *In vitro* cell compatibility

The viability of HDFs and A549 cells cultured in a medium where the hydrogel was previously suspended and swelled was evaluated.

Table 1
Thiolated chitosan characterization and composition of hydrogel.

Sample	CS:NAC:HOBt:EDAC (molar ratio)	–SH ($\mu\text{mol/g}$)	–SH:–acrylate (molar ratio)
CS–NAC1	1:2:1:4	361.4 ± 15.0	1:1
CS–NAC2	1:2:1:8	221.0 ± 12.4	1:1 1:2 1:5

In particular, the hydrogel was incubated in Dulbecco's modified Eagles medium (DMEM) at 37 °C for 5 d under orbital stirring at 120 rpm. After incubation, the medium “conditioned” by the hydrogel, was centrifuged at 11800 rpm, 4 °C for 30 min, and then filtered to remove the hydrogel. The cells were seeded into 96-well plates at 10,000 cells per well. The plates were then returned to the incubator and the cells were allowed to grow to confluence for 24 h. Subsequently, the culture medium was replaced with the “conditioned” medium. After 3 d and 7 d of incubation (37 °C, 5% CO₂), 20 μL of MTT solutions were used to replace the mixture in each well. The plates were then returned to the incubator and incubated for a further 4 h in 5% CO₂ at 37 °C. Then, the culture medium and MTT were removed. Isopropanol (150 μL) was then added to each well to dissolve the formazane crystals. The plate was placed in 5% CO₂ at 37 °C for 10 min and for 15 min at 6 °C before measurement. The optical density was read on a microplate reader at 570 nm. Cell viability was determined as a percentage of the negative control (untreated cells). Each experiment was performed in triplicate and results are reported as mean standard deviation.

3. Results and discussion

3.1. Synthesis and characterization of CS–NAC

CS–NAC was achieved by the covalent attachment of NAC to the amine groups of CS. The coupling reaction was mediated by EDAC and HOBt as we have previously reported [43]. And the amount of immobilized thiol groups was strongly dependent on the molar ratio of reagents (CS, NAC, HOBt and EDAC). Particularly, NAC/EDAC molar ratio significantly influenced the amount of thiol group per gram polymer. In the present research, we used two kinds of NAC/EDAC molar ratios and Ellman's tests showed the contents of free thiol group were 361.4 and 221.0 $\mu\text{mol/g}$, respectively (Table 1).

3.2. In situ formation and characterization of hydrogel

Upon exposure to air, the thiols on CS–NAC are oxidized to form a spontaneous, albeit slow, disulfide-crosslinked hydrogel (CN hydrogel). Then, to enhance the rate of cross-linking, hydrogels were formed in situ via Michael type addition between CS–NAC and

PEGDA in PBS at pH 7.4 and 37 °C (CNP hydrogel, Fig. 1). The concentration is defined as the dry weight of CS–NAC per volume of buffer.

Table 2 shows the gelation time of hydrogels with different compositions and concentrations. As can be seen, the gelation time of CNP hydrogel was much shorter than that of CN hydrogel. Indeed, Michael type addition between thiol group and acrylate group has a faster rate than the spontaneous oxidation of thiols [44]. For CNP hydrogel, at the same concentration and molar ratio of thiol to acrylate, the gelation time decreased from 45 to 30 min with increasing the content of free thiols from 221.0 to 361.4 $\mu\text{mol/g}$, and the tendency is the same as CN hydrogel. The results indicate that Michael type addition or the spontaneous oxidation was easier to process as the content of free thiols increased. Then, for CNP2 hydrogel at the same concentration, the gelation time decreased from 45 to 25 min with decreasing the molar ratio of thiol to acrylate from 1:1 to 1:5, indicating that the increasing amounts of PEGDA enhanced the rate of cross-linking between thiol and acrylate group and consequently shortened the gelation time [24]. For CNP2 (1:1) hydrogel, the gelation time decreased from 55 to 27 min by increasing the concentration from 5 to 15 mg/mL, which was in agreement with the results described by Hiemstra et al. [26,27]. For CNP2 (1:1) hydrogel at the same concentration, the gelation time was prolonged from 45 to 130 min by decreasing the temperature from 37 to 25 °C, indicating that Michael type addition preferred to go under physiological temperature. In general, the gelation time of hydrogels achieved by Michael type addition was short in comparison with those by the spontaneous oxidation and can be modulated by the concentration of CS–NAC and PEGDA, the content of free thiols in CS–NAC, and the temperature.

Fig. 2 shows X-ray diffraction profiles of CS–NAC and CNP hydrogel. For CS, at least seven polymorphs have been proposed [45–47], including “tendon–CS”, “annealed”, “I-2”, “L-2”, “form I”, “form II”, and “noncrystalline”. Pocker and Biswas have proposed three forms: noncrystalline, hydrated (“tendon”) crystalline, and anhydrous (“annealed”) crystalline [48]. The hydrated crystalline structure gives a reflection at $2\theta = 10^\circ$ (or peaks at around 8° and 12°), and the anhydrous crystalline structure gives one at $2\theta = 15^\circ$. Fig. 2 illustrates CS shows characteristic peaks around $2\theta = 12.6^\circ$, 19° , and 26° [49]. The former peak corresponded to the hydrated crystalline structure, while the broaden peak around $2\theta = 21^\circ$ for CS–NAC indicated the existence of an amorphous structure, suggesting that the introduction of NAC changed the crystalline structure of CS. The crystalline PEG shows strong reflections at 18.74° and 22.86° and weak reflections at 26.77° , 30.5° , 35.9° , and 40° . In the CNP hydrogel, the 12.6° reflection for CS is absent, and there is a broad peak in the 18 – 26° region, which may have contributions from both CS and PEG. This indicates that there was a decrease in CS crystallization upon the introduction of PEG. As the PEG content in CNP hydrogel increases, the intensity of characteristic reflections

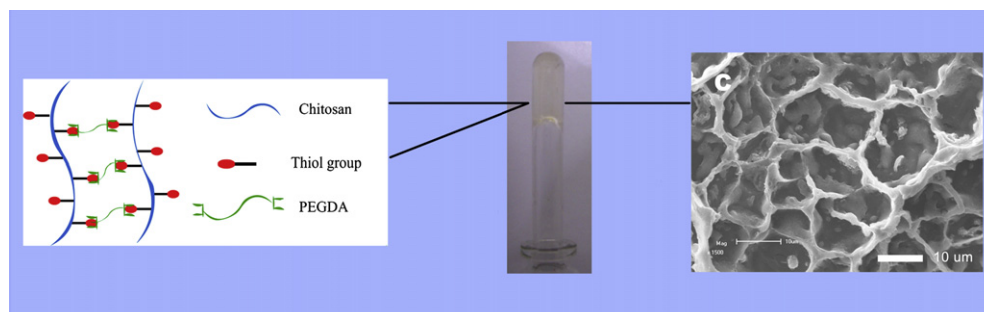


Fig. 1. Demonstration of the in situ hydrogel formation.

Table 2

Gelation time as function of composition and concentration of hydrogel.

	CN1 ^a	CN2 ^a	CNP1 (1:1) ^b	CNP2 (1:1) ^b	CNP2 (1:1) 25 °C ^{b,c}	CNP2 (1:2) ^b	CNP2 (1:5) ^b
Concentration (mg/mL)	10	10	10	5	10	15	10
Gelation time (min) ^d	145 ± 15	180 ± 16	30 ± 4	55 ± 5	45 ± 4	27 ± 4	130 ± 13

^a CN corresponds to the hydrogel achieved by CS–NAC.^b CNP corresponds to the hydrogel achieved by CS–NAC and PEGDA.^c CNP2 (1:1) 25 °C corresponds to the CNP2 (1:1) hydrogel which was formed at 25 °C. And all the other hydrogels showed in table were formed at 37 °C.^d The gelation time was determined by a flow test utilizing a test tube inverting method.

from the resulting hydrogel increased. It is natural that the high content of PEG can lead to larger amounts of crystalline structures in the hydrogel [50].

Thermal stabilities of CS, CS–NAC and CNP hydrogel were measured using TGA analysis. Fig. 3 shows the weight loss and weight loss rate curves recorded with a heating rate of 10 °C/min in nitrogen between 20 and 650 °C. CS and CS–NAC showed single stage thermal decomposition at about 250 °C, indicating that thiol-modified did not affect the thermal stability of CS. However, all the CNP hydrogels showed a two-stage thermal decomposition. The first-stage decomposition temperature was also about 250 °C, suggesting the introduction of PEG via Michael type addition did not decrease thermal stability of CS, compared with the incorporation of PEG via a traditional epoxy–amine reaction [50]. Furthermore, the second-stage decomposition temperature was approximately 380 °C and the weight loss for CNP2 (1:1), CNP2 (1:2) and CNP2 (1:5) was 10%, 23% and 50%, respectively. The weight loss results were similar to the contents of PEG in CNP hydrogel and indicate that the decomposition stage was caused by PEG. In particular, as the molar ratio of thiol to acrylate decreasing from 1:1 to 1:5, the degradation temperature increased from 357.5 to 388.6 °C, this is probably due to the high content of PEG promoting the crystal growth of the hydrogel [51], which had been demonstrated by X-ray diffraction.

The morphologies of the swollen CN and CNP hydrogel in PBS at 37 °C for different time periods were observed by SEM. As shown in Fig. 4A–D, the SEM images of hydrogels exhibited a highly macroporous spongelike structure and the average mesh size is about 10 μm. With the increasing of cross-linking density, the decrease of the pore size was attributed to the decreasing distance between CS chains with increasing PEGDA concentration. After being dipped in PBS for 24 h and 7 d, the chains in the network degraded and the

pores of the hydrogel increased (Fig. 4E–H). The porous structure of the hydrogel shows potential as scaffolds for cell infiltration and growth.

3.3. Rheology

Oscillatory stress sweep allows determination of the linear viscoelastic region (LVR) profiles and storage modulus (G') of the hydrogels as a function of the content of free thiols, concentration and the ratio of thiol to acrylate (Fig. 5A). As can be seen, with increasing cross-linking density of the hydrogel, the structure breakdown occurred at higher shear stress levels. On the basis of these data, a stress 10 Pa was chosen for comparison of various hydrogel samples. Indeed, numerous published reports have

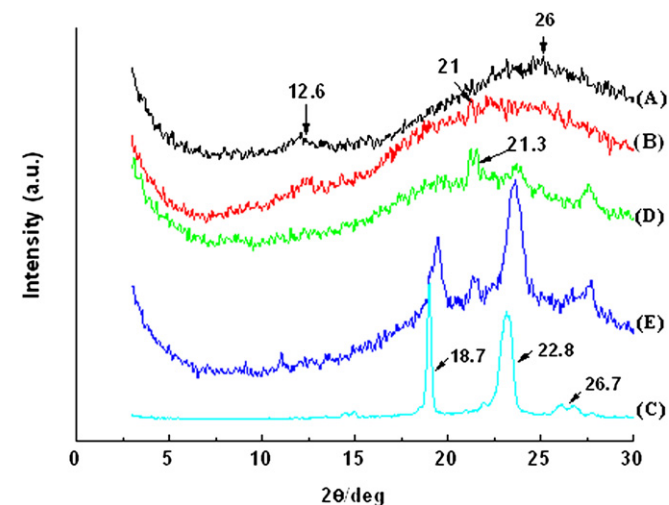
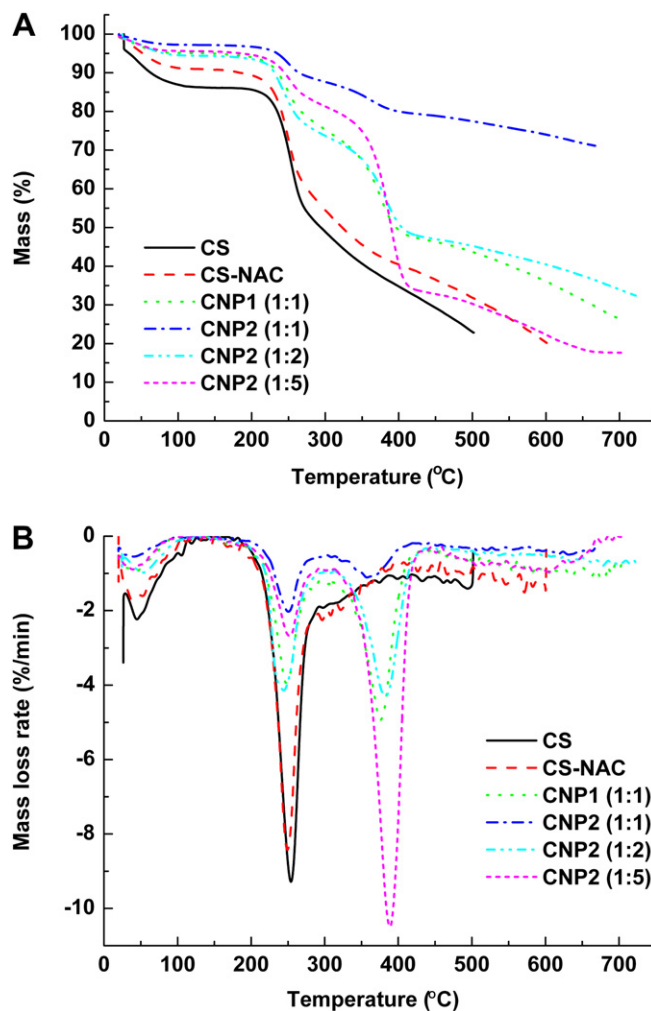


Fig. 2. X-Ray diffraction patterns for chitosan (A), chitosan–NAC (B), PEGDA (C), CNP2 (1:1) hydrogel (D), and CNP2 (1:5) hydrogel (E).

Fig. 3. Thermogravimetric analysis of chitosan, chitosan–NAC, and CNP hydrogels. (A) the weight loss curves, (B) the weight loss rate curves.

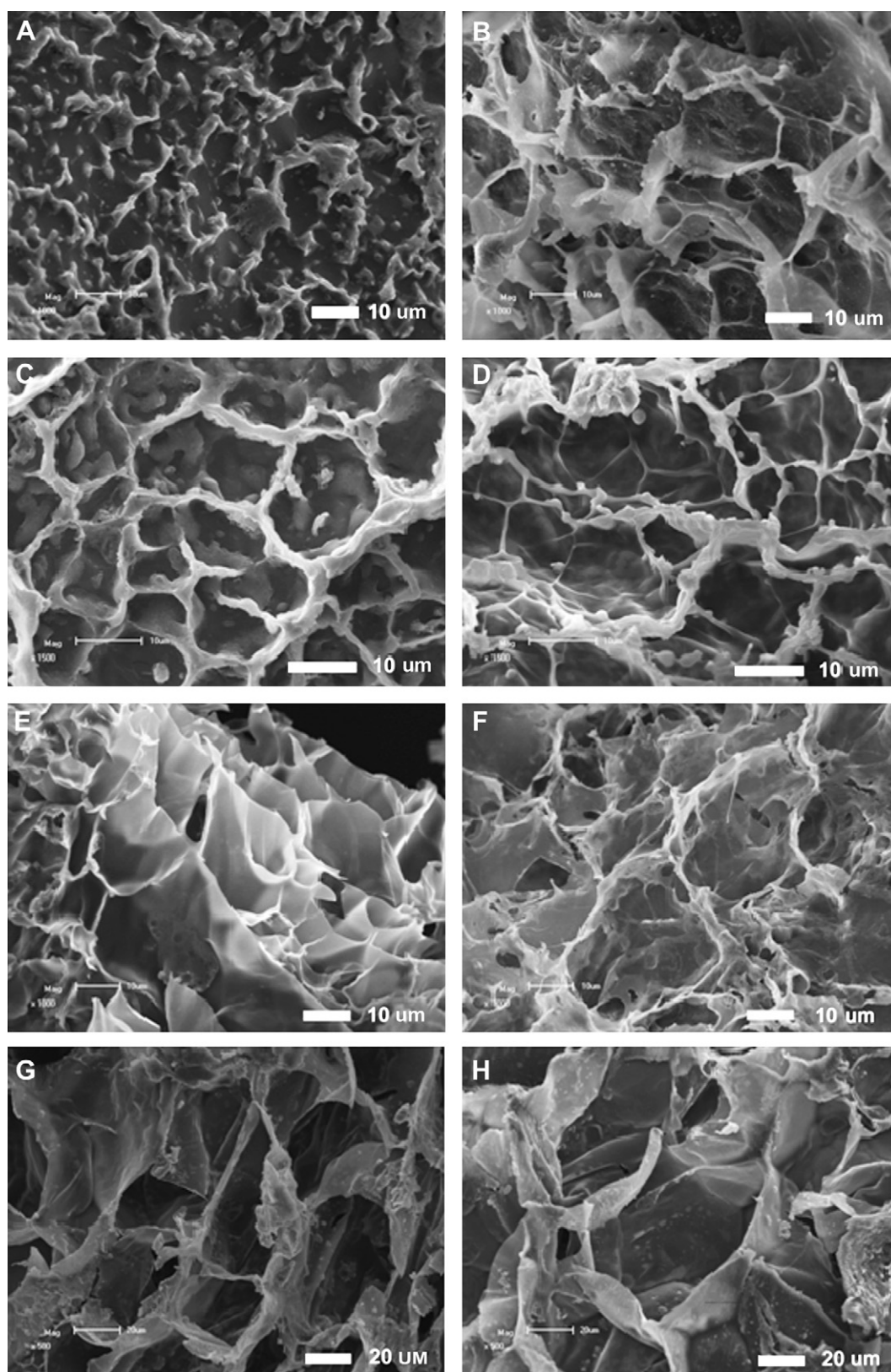


Fig. 4. SEM photographs of (A) CN hydrogel, (B) CNP1 (1:1) hydrogel, (C) CNP2 (1:1) hydrogel, and (D) CNP2 (1:5) hydrogel dipped in water for 0.5 h at 37 °C; (E) CNP1 (1:1) hydrogel and (F) CNP2 (1:1) hydrogel for 24 h at 37 °C; (G) CNP1 (1:1) hydrogel and (H) CNP2 (1:1) hydrogel for 7 days at 37 °C.

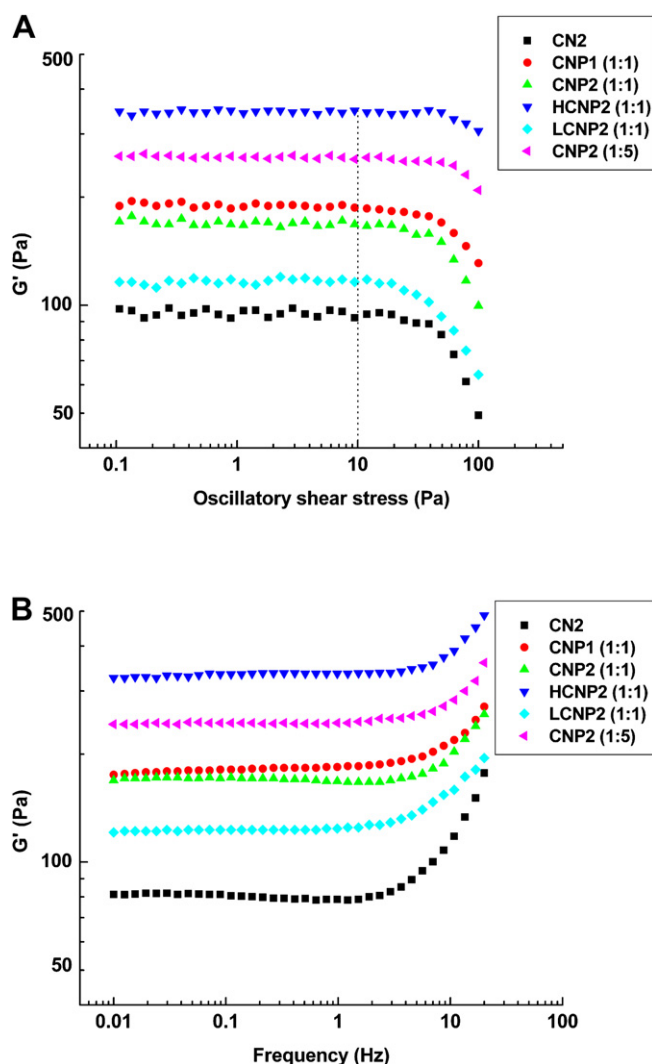


Fig. 5. Rheological behaviors of various hydrogel samples. (A) Oscillatory shear stress sweep, (B) oscillatory frequency sweep. HCNP2 (1:1): CNP2 (1:1) hydrogel at high concentration (15 mg/mL); LCNP2 (1:1): CNP2 (1:1) hydrogel at low concentration (5 mg/mL).

suggested that the measured G' has a strong relationship to the number of effective intermolecular cross-links formed in the hydrogel network [52–54]. Therefore, the evolution of G' as a function of cross-linking density was monitored to assess the extent of effective intermolecular cross-links formed in the hydrogel networks. As we can see, all the CNP hydrogels have a higher G' than CN hydrogel, indicating that the introduction of PEG via Michael type addition increased the cross-linking density. Then, for the CNP hydrogel, the higher cross-linking density and elasticity of hydrogel can be achieved by increasing the contents of free thiols in CS–NAC and decreasing molar ratio of thiol to acrylate. For the CNP hydrogel with different concentration, the higher concentration of CS–NAC made the achieved hydrogel having a higher cross-linking density, suggesting that increasing the concentration of CS–NAC can get a higher content of free thiols under the same volume.

Frequency sweep tests are widely used to obtain information about the stability of three-dimensional cross-linked networks [52,55,56]. Fig. 5B shows the plot between G' and oscillatory frequency, the data obtained for all the hydrogels is characterized by G' exhibiting a plateau in the range of 0.01–2 Hz that is indicative of a stable, cross-linked network. However, at higher frequencies

(2–20 Hz), all the hydrogels showed an increase in G' , and the higher cross-linking density made higher rate of increase. The magnitude of viscoelastic response elicited by a polymeric network is governed primarily by the length of the flexible polymer chains and the nature of the imposed mechanical motion [52,55]. Longer chains have characteristic longer relaxation times and cause a low cross-linking density in the hydrogel network. At higher frequencies, long chains fail to rearrange themselves in the time scale of the imposed motion and therefore stiffen up, which was characterized by a sharp increase in G' .

3.4. Hydrogel swelling

To study the swelling and degradation of hydrogel, the prepared hydrogel was dried under vacuum at room temperature to a constant weight, and then the dried hydrogel was immersed into PBS and allowed to swell at 25 or 37 °C. All the hydrogels swelled rapidly and reached equilibrium within 0.5 h at 37 °C, but within 4 h at 25 °C (Supporting Information). Fig. 6 shows the equilibrium swelling ratio of CN and CNP hydrogels. For CNP2 (1:1) hydrogel at different concentrations, the equilibrium swelling ratio decreased from 1336% to 888% when increasing the concentration from 5 to 15 mg/mL (Fig. 6A), indicating that the hydrogel prepared at a high concentration has a tighter structure and a lower water-holding capacity than at a low concentration. For CNP2 hydrogel at different molar ratio of thiol to acrylate, the equilibrium swelling ratio decreased from 1195% to 568% by decreasing the molar ratio of thiol to acrylate from 1:1 to 1:5 (Fig. 6B), suggesting that the construction of the hydrogel with a higher content of PEG was too tight to hold water. For CNP hydrogel at same condition, the equilibrium swelling ratio decreased from 1195% to 907% when increasing the content of free thiols from 221.0 to 361.4 $\mu\text{mol/g}$ (Fig. 6C), implying the high content of free thiols caused a tight network structure of the hydrogel. For CN hydrogel with different contents of free thiols, the equilibrium swelling ratios were similar and lower than all the CNP hydrogels (Fig. 6C). The results indicate that the thiol oxidation in the CN hydrogel was similar, as well as the construction of hydrogel. Moreover, there was a longer distance between the CS chains in CNP hydrogel than CN hydrogel due to the introduction of PEG moieties, so CN hydrogel has a tight network structure compared to CNP hydrogel.

Furthermore, the equilibrium swelling ratios of CNP hydrogels were higher at 37 °C than at 25 °C compared to CN hydrogel. The phenomenon was in good agreement with the results described by El-Sherbiny et al. [57] and Khurma et al. [58], indicating the temperature-responsive behavior of CNP hydrogel. This behavior is due to the dissociation of the hydrogen bond in chitosan within the hydrogel matrices at higher temperature and thus allowing more water to move into the matrix of hydrogel [59].

The CN and CNP hydrogels were degradable under physiological conditions. There are two kinds of degradation in CNP hydrogels. One is the degradation through hydrolysis of the ester bond between the thioether and PEG, as the hydrogels via Michael type addition [23–28]; the other is the biodegradation of CS. Indeed, CS can be easily depolymerized by a variety of hydrolases including lysozyme, pectinase, cellulases, hemicellulases, lipases, and amylases [29]. After reaching swelling equilibrium, all the hydrogels were rapidly degraded in the first 24 h, and then the degradation became slow and the persistence of hydrogel remnants was also observed within six weeks (Supporting Information).

3.5. In vitro cell compatibility

The biocompatibility of CN and CNP hydrogels was evaluated *in vitro* on HDFs and A549 cells by “indirect” methods. In this method, the growth medium was first “conditioned” for 5 d with the

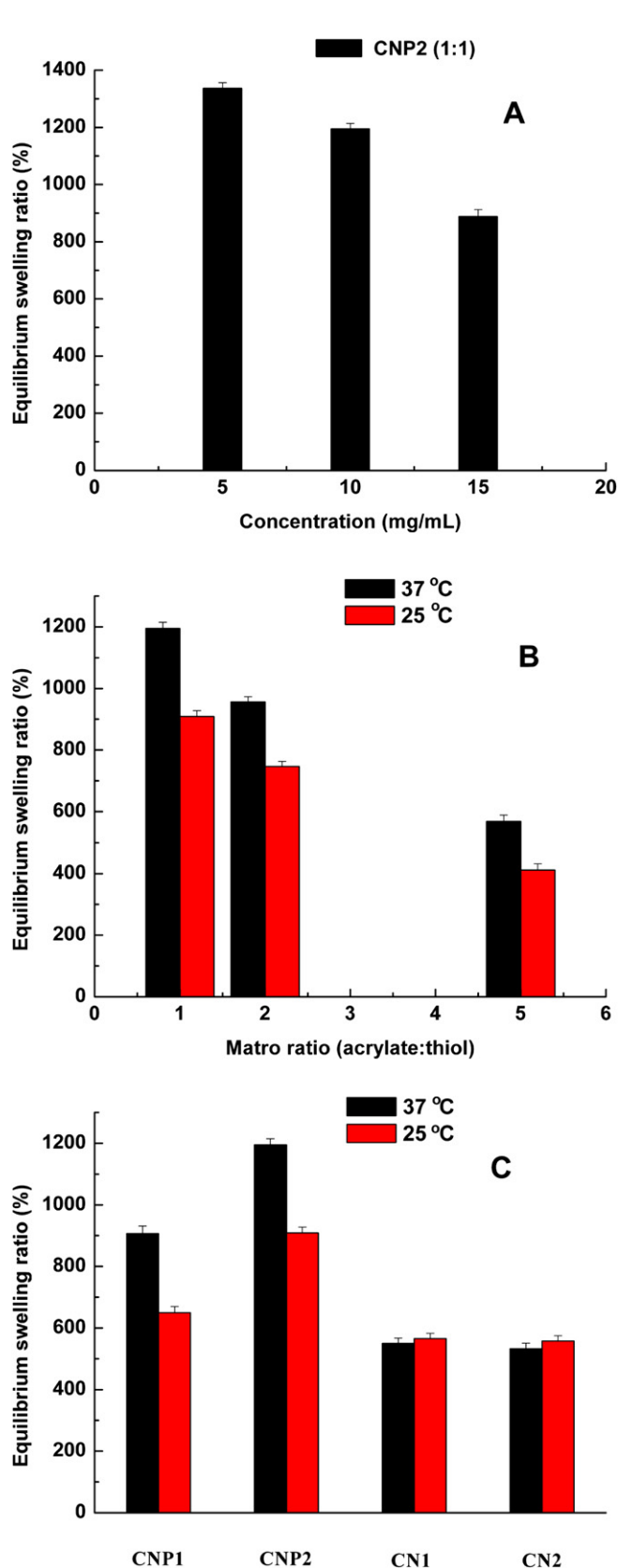


Fig. 6. Equilibrium swelling ratio of CN and CNP hydrogels under different conditions. (A) CNP2 (1:1) hydrogels under different concentration, (B) CNP2 hydrogels under different temperature and molar ratio of acrylate to thiol, (C) CN and CNP hydrogel under different temperatures.

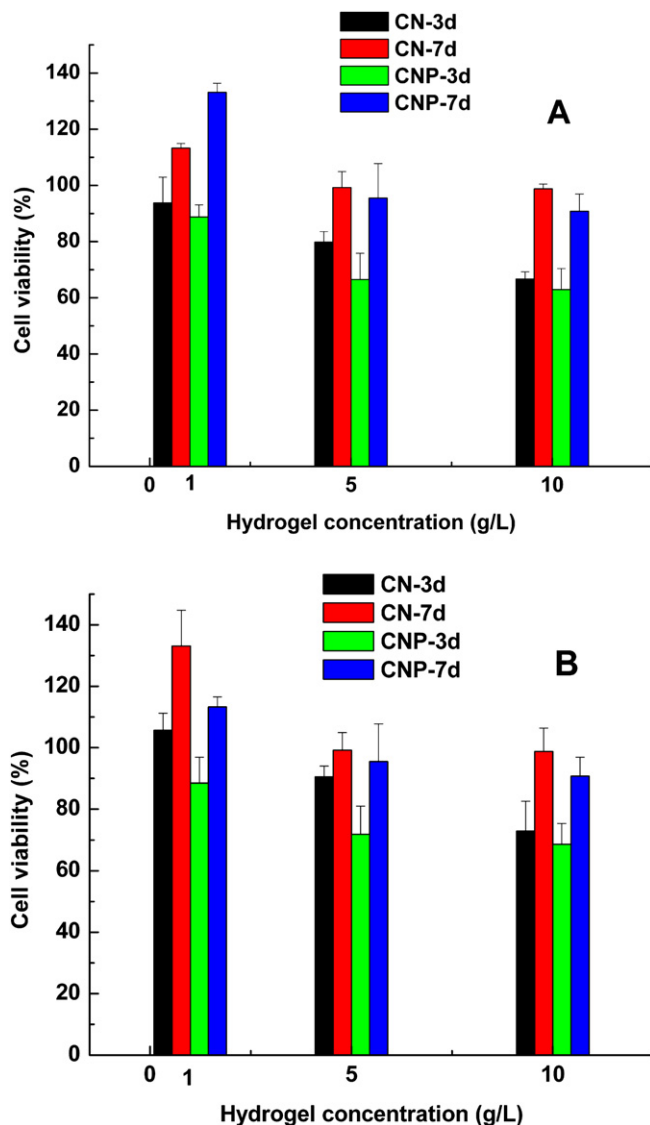


Fig. 7. Cell viability (MTT assays) for HDFs (A) and A549 (B) cells grown on CN2 and CNP2 (1:1) hydrogels.

hydrogel and then used to incubate the cells. After 3 and 7 d of incubation, cell viability was determined by the MTT assay and expressed as a percentage ratio between viable cell number incubated in the growth medium “conditioned” and not “conditioned” by the hydrogel.

Fig. 7 shows cell viability (MTT assay) of CN2 and CNP2 hydrogels with different cells and incubated time. As can be seen, for two different cell types, the cell viability of CNP hydrogel was a little lower than that of CN hydrogel after 3 d incubated, which may be due to the rapid degradation of CNP hydrogel, and the degraded segment of hydrogel may contain some substances that interfere with the cell viability. And the cells appeared to be recovered by 7 d, all the cell viabilities were maintained over 80%. These properties suggest that the CNP hydrogel has many potential clinical applications in drug delivery and tissue engineering.

4. Conclusion

Thiol-modified chitosan with the contents of free thiol groups 361.4 and 221.0 $\mu\text{mol/g}$ was conveniently prepared by a one-pot synthesis procedure at room temperature. Hydrogels were rapidly

formed *in situ* under physiological conditions by Michael type addition upon mixing aqueous solutions of CS–NAC and (PEGDA) at different concentrations and ratios of thiol to acrylate. Their mechanical and swelling properties are readily controlled by the content of free thiols in CS–NAC, temperature, and concentration of CS–NAC and PEGDA. The hydrogels were degradable under physiological conditions. *In vitro* cell compatibility study on HDFs and A549 cells indicates CNP hydrogel has good compatibility. These hydrogels present great potential in biomedical applications including drug delivery, as well as injectable tissue engineered scaffolds.

Acknowledgments

This work was supported in part by the National Natural Science Foundation of China (Grant No. 20804021), the Natural Science Foundation of Tianjin (Grant No. 08JCYBJC00300), the Ph.D. Programs Foundation for New Teachers of Ministry of Education of China (Grant No. 200800551030), and Tianjin Health Bureau Scientific Research Found (07kz47) are gratefully acknowledged.

Appendix. Supplementary data

Supplementary information associated with this article could be found on-line, at doi:10.1016/j.polymer.2009.12.003.

References

- [1] Hoffman AS. *Adv Drug Deliv Rev* 2002;43:3–12.
- [2] Peppas NA, Hilt JZ, Khademhosseini A, Langer R. *Adv Mater* 2006;18:1345–60.
- [3] Hoare TR, Kohane DS. *Polymer* 2008;49:1993–2007.
- [4] Lee KY, Mooney DJ. *Chem Rev* 2001;101(7):1869–79.
- [5] Nuttelman CR, Rice MA, Rydholm AE, Salinas CN, Shah DN, Anseth KS. *Prog Polym Sci* 2008;33:167–79.
- [6] Hatefi A, Amsden B. *J Control Release* 2002;80:9–28.
- [7] Packhaeuser CB, Schnieders J, Oster CG, Kissel T. *Eur J Pharm Biopharm* 2004;58:445–55.
- [8] Kretlow JD, Klouda L, Mikos AG. *Adv Drug Deliv Rev* 2007;59:263–73.
- [9] Van Tomme SR, Storm G, Hennink WE. *Int J Pharm* 2008;355:1–18.
- [10] He CL, Kim SW, Lee DS. *J Control Release* 2008;127:189–207.
- [11] Sawhney AS, Pathak CP, Hubbell JA. *Macromolecules* 1993;26:581–7.
- [12] Mi FL, Shyu SS, Wong TB, Jang SF, Lee ST, Lu KT. *J Appl Polym Sci* 1999;74:1093–107.
- [13] Kuo CK, Ma PX. *Biomaterials* 2001;22:511–21.
- [14] Van Tomme SR, van Steenberg MJ, De Smedt SC, van Nostrum CF, Hennink WE. *Biomaterials* 2005;26:2129–35.
- [15] Huang X, Lowe TL. *Biomacromolecules* 2005;6:2131–9.
- [16] Haines-Butterick L, Rajagopal K, Branco M, Salick D, Rughani R, Pilarz M, et al. *Proc Natl Acad Sci U S A* 2007;104:7791–6.
- [17] Choi HS, Yui N. *Prog Polym Sci* 2006;31:121–44.
- [18] Qiu B, Stefanos S, Ma J, Lalloo A, Perry BA, Leibowitz MJ, et al. *Biomaterials* 2003;24:11–8.
- [19] Tae G, Kim YJ, Choi WI, Kim M, Stayton PS, Hoffman AS. *Biomacromolecules* 2007;8:1979–86.
- [20] Metters A, Hubbell JA. *Biomacromolecules* 2005;6:290–301.
- [21] Van de Wetering P, Metters AT, Schoenmakers RG, Hubbell JA. *J Control Release* 2005;102:619–27.
- [22] Rizzi SC, Hubbell JA. *Biomacromolecules* 2005;6:1226–38.
- [23] Shu XZ, Ghosh K, Liu YC, Palumbo FS, Luo Y, Prestwich GD, et al. *J Biomed Mater Res* 2004;68A:365–75.
- [24] Ghosh K, Shu XZ, Mou R, Lombardi J, Prestwich GD, Rafailovich MH, et al. *Biomacromolecules* 2005;6:2857–65.
- [25] Shu XZ, Ahmad S, Liu YC, Prestwich GD. *J Biomed Mater Res* 2006;79A:902–12.
- [26] Hiemstra C, van der Aa LJ, Zhong Z, Dijkstra PJ, Feijen J. *Macromolecules* 2007;40:1165–73.
- [27] Hiemstra C, van der Aa LJ, Zhong Z, Dijkstra PJ, Feijen J. *Biomacromolecules* 2007;8:1548–56.
- [28] Hiemstra C, Zhong Z, van Steenberg MJ, Hennink WE, Feijen J. *J Control Release* 2007;122:71–8.
- [29] Ravi Kumar MNV, Muzzarelli RAA, Muzzarelli C, Sashiwa H, Domb AJ. *Chem Rev* 2004;104:6017–84.
- [30] Sashiwa H, Aiba S. *Prog Polym Sci* 2004;29:887–908.
- [31] Rinaudo M. *Prog Polym Sci* 2006;31:603–32.
- [32] Gingras M, Paradis I, Berthod F. *Biomaterials* 2003;24:1653–61.
- [33] Wang YC, Lin MC, Wang DM, Hsieh HJ. *Biomaterials* 2003;24:1047–57.
- [34] Francis Suh JK, Matthew HWT. *Biomaterials* 2000;21:2589–98.
- [35] Bhattarai N, Ramay HR, Gunn J, Matsen FA, Zhang MQ. *J Control Release* 2005;103:609–24.
- [36] Bhattarai N, Matsen FA, Zhang MQ. *Macromol Biosci* 2005;5:107–11.
- [37] Wua J, Wei W, Wang LY, Su ZG, Ma GH. *Biomaterials* 2007;28:2220–32.
- [38] Zhang XG, Zhang HJ, Wu ZM, Wang Z, Niu HM, Li CX. *Eur J Pharm Biopharm* 2008;68:526–34.
- [39] Kim M-S, Choi Y-J, Noh I, Tae G. *J Biomed Mater Res* 2007;83A:674–84.
- [40] Cruise GM, Scharp DS, Hubbell JA. *Biomaterials* 1998;19:1287–94.
- [41] Krauland AH, Hoffer MH, Bernkop-Schnürch A. *Drug Dev Ind Pharm* 2005;31:885–93.
- [42] Jeong B, Bae YH, Kim SW. *Macromolecules* 1999;32:7064–9.
- [43] Wang X, Zheng C, Wu Z, Teng D, Zhang X, Li C, et al. *J Biomed Mater Res Part B Appl Biomater* 2009;88B:150–61.
- [44] Shu XZ, Liu YC, Palumbo FS, Luo Y, Prestwich GD. *Biomaterials* 2004;25:1339–48.
- [45] Ogawa K, Hirano S, Miyamishi T, Yui T, Watanabe T. *Macromolecules* 1984;17:973–5.
- [46] Saito H, Ryoko T, Ogawa K. *Macromolecules* 1987;20:2424–30.
- [47] Samuels RJ. *J Polym Sci Polym Phys Ed* 1981;19:1081–105.
- [48] Pocker Y, Biswas SB. *Biochemistry* 1980;19:5043–9.
- [49] Radhakumary C, Nair PD, Reghunadhan Nair CP, Mathew S. *J Appl Polym Sci* 2009;114:2873–86.
- [50] Kiuchi H, Kai W, Inoue Y. *J Appl Polym Sci* 2008;107:3823–30.
- [51] Zhao W, Yu L, Zhong X, Zhang Y, Sun J. *J Macromol Sci Phys* 1995;B34(3):231–5.
- [52] Anseth KS, Bowman CN, Brannon-Peppas L. *Biomaterials* 1996;17:1647–57.
- [53] Santovena A, Alvarez-Lorenzo C, Concheiro A, Llabres M, Farina JB. *Biomaterials* 2004;25:925–31.
- [54] Lee KY, Bouhadir KH, Mooney DJ. *Biomaterials* 2004;25:2461–6.
- [55] Kavanagh GM, Ross-Murphy SB. *Prog Polym Sci* 1998;23:533–62.
- [56] Lutolf MP, Hubbell JA. *Biomacromolecules* 2003;4:713–22.
- [57] El-Sherbiny IM, Abdel-Bary EM, Harding DRK. *J Appl Polym Sci* 2006;102:977–85.
- [58] Khurma JR, Nand AV. *Polym Bull* 2008;59:805–12.
- [59] Kim SJ, Park SJ, Kim SI. *React Funct Polym* 2003;55:53–9.